$H\cdot(H_2O)_n$ Clusters: Microsolvation of the Hydrogen Atom via Molecular ab Initio Gradient Embedded Genetic Algorithm (GEGA)

Anastassia N. Alexandrova*

Department of Chemistry and Biochemistry, University of California, Los Angeles, Los Angeles, California, 90095-1569

Received: September 28, 2010; Revised Manuscript Received: October 27, 2010

A new version of the ab initio gradient embedded genetic algorithm (GEGA) program for finding the global minima on the potential energy surface (PES) of mixed clusters formed by molecules and atoms is reported. The performance of the algorithm is demonstrated on the neutral $H\cdot(H_2O)_n$ ($n = 1-4$) clusters, that is, a radical H atom solvated in 1−4 water molecules. These clusters are of a fundamental interest. The solvated hydrogen atom forms during photochemical events in water, or during scavenging of solvated electrons by acids, and transiently exists in biological systems and possibly in inclusion complexes in the deep ocean and in the ice shield of earth. The processes associated with its existence are intriguingly complex, however, and have been the subject of decades-long debates. Using GEGA, we explicate the apparently extreme structural diversity in the $H\cdot(H_2O)_n$ ($n = 1-4$) clusters. All considered clusters have four basic structural types: type **I**, where the H radical is weakly coordinated to the oxygen atom of one of the water molecules; type **II**, where H is weakly coordinated to a H atom of one of the water molecules; type **III**, consisting of H_2, the OH radical, and $n - 1$ H_2O molecules; and type **IV**, consisting of H_3O and $n - 1$ H_2O. There are myriads of isomers of all four types. The lowest energy species of types **I** and **II** are the isoenergetic global minima. $H\cdot(H_2O)_n$ clusters appear to be a challenging case for GEGA because they have many shallow minima close in energy some of which are significantly less stable than the global minimum. Additionally, the global minima themselves have high structural degeneracy, they are only weakly bound, and they are prone to dissociation. GEGA performed exceptionally well in finding both the global and the low-energy local minima that were subsequently confirmed at higher levels of theory.

Introduction

Finding the global minimum structures on potential energy surfaces (PESs) is one of the fundamental physicochemical problems. It is part of the bigger question of calculating the partition function of a chemical system, especially at finite temperatures, that would fully describe the state of a system. For many chemical systems, including gas-phase clusters, solids, molecules, macromolecules, and interfaces, potential energy landscapes are very complicated. As a result, manual search procedures become highly unreliable creating demand for automated procedures based on human-unbiased algorithms. Over recent years, several algorithms emerged for global minimum searches. The most traditional method for this task is the method of the Monte Carlo (MC) annealing.[1] MC guarantees the correctness of the found global minimum but in exchange for an enormous amount of stochastic sampling of the conformational space. Among other most prominent stochastic methods, there are the basin-hopping method,[2] the kick technique by Saunders[3] or the similar random search and minimization technique by Lloyd and Johnston,[4] multicanonical methods,[5] minima hopping,[6] and the particle swarm algorithm.[7] Occasionally, molecular dynamics is used for finding the structure of the system, but in general, this does not guarantee that the global minimum is found; instead, that which is found is often simply a local minimum nearest to the starting geometry of the system. There is also a separate group of semistochastic genetic algorithm (GA) methods,[8,9] which are based on Darwinian-like gradual optimization of the population of structures by setting them to exchange structural information and to pass it on to offspring. GA techniques are among the most powerful, if not the most powerful, precisely because there is an incorporated memory effect such that the learned good structural information is not lost but is recycled in the sampling of the configurational space, and yet there is a way to diversify the population by acquisition of new structural features via mutations.

We recently developed an efficient GA method additionally facilitated by following the ab initio gradient on the PES. Specifically, every structure participating in the GA procedure is ensured to be a local minimum through geometry optimization and vibrational frequency analysis. This method, called ab initio gradient embedded genetic algorithm (GEGA),[9] proved to be exceptionally successful in finding the global and the low-energy local minima on the PES of atomic clusters.[10] GEGA converges in only a few dozen of GA iterations (compared to hundreds of iterations required in conventional GAs on the basis of single-point energy calculations). Also, GEGA produces geometries and relative energies of isomers with ab initio quality. Here, we present a new version of GEGA with the developed capability of operating on clusters formed by both molecules and atoms. Using the new GEGA, we explore the ground PES of the $H\cdot(H_2O)_n$ clusters, which appear to be a tough test case for the algorithm because of the apparent topography of the PES. Nonetheless, the new GEGA proved itself to be an instrumental and accurate tool for the meticulous exploration of PESs and for finding the global and low-lying local minima.

* E-mail: ana@chem.ucla.edu.

10.1021/jp1092543
Published on Web 11/15/2010

The system of interest, a single hydrogen atom solvated in water, is one of the fundamental entities on earth. It transiently exists in biology, for example, in certain enzymes exhibiting the proton-coupled electron transfer (PCET) between a single donor and a single acceptor.[11,12] Trapping of hydrogen atom in clathrate cages in the deep ocean and in the ice shield of earth is also possible.[13] Solvated H forms during scavenging of solvated electrons with acids.[14] It is also relevant to photochemical processes in water.[15] As elaborated below, unavoidably, the processes associated with the presence of this simplest hydrophobic solute in water are complex and are often nonadiabatic, that is, occurring on multiple potential energy surfaces. The $H\cdot(H_2O)_n$ clusters represent the simplest model for hydrated H, which allows for the assessment of properties of this system at a fundamental level.

The $H\cdot(H_2O)_n$ clusters and the H solvated in bulk water are relevant to the processes of the formation of the solvated electron, which is an entity that has received an enormous amount of attention in the literature. Specifically, the H radical can reversibly dissociate in water to form a proton and an electron. The solvated electron can be stabilized when a proton is abstracted from H by a base, for example, a hydroxyl anion. This was predicted, for example, in a kinetic electron paramagnetic resonance (EPR) study.[16] The reaction of recombination between H and OH^- is rather slow and was demonstrated to have two different kinetic regimes at temperatures below and above 100 °C.[17] On the basis of this unusual behavior, a nonadiabatic and PCET nature of the process was suspected. A recent density functional theory (DFT) molecular dynamics study suggested that H^+ transfer and the preceding diffusion of the H radical in water both contribute to the lag in the time of recombination of H with OH^-.[18]

For the reverse reaction of electron−proton recombination, it has been debated whether the proton or the electron migration governs the process. The reaction does not proceed under diffusion control and has a large isotope effect.[19] Furthermore, surprisingly, the diffusion of H in water was shown to be similarly facile to that of H^+ in water, although the mechanisms of the two processes have to be very different.[20] A Car−Parrinello molecular dynamics study[13] explained this observation by the proposal that H diffuses together with its water cavity, which is facilitated by rapid water exchanges due to H-bonding fluctuations. An ab initio molecular dynamics study of recombination of a solvated H^+ and an electron showed that the process is driven by the diffusion of H^+ and the distortion of the solvated electron.[21] Thus, most recently, this mechanistic argument has settled on the major role of H^+ migration in the mechanism.

The solvated H_3O radical and the $H_3O\cdot OH^-$ complex were also claimed to be relevant to the presence of the solvated electron in water.[15,22−26] For example, it was shown that the absorption spectra of H_3O solvated by different numbers of water molecules cover the range of that of the hydrated electron.[15,27] The resonance Raman spectra of $H_3O\cdot(H_2O)_n$ also converge to that of the solvated electron as n increases.[22] Furthermore, a solvated electron can recombine with H_3O^+.[16] This reaction is again more likely to proceed via H^+ transfer from H_3O^+ to the electron rather than via electron transfer to H_3O^+.[16] A relevant reaction, $H + H_2O \rightarrow H_2 + OH$, was thoroughly investigated through multireference ab initio calculations.[28] In particular, it was shown that there are six different possible configurations of the system on the ground PES including those containing OH and H_2 in various mutual orientations, the HOHH molecule, and the H_3O radical. An ab initio and density functional theory (DFT) study predicted that H_3O and OH can barrierlessly form from water on its S1 excited state PES.[15] Hence, H_3O should emerge during photochemical processes in water. On the ground PES, however, solvated H_3O is a metastable minimum separated only by a small barrier of a few kcal/mol from the ejection of H or H_2 at least for certain numbers of solvent water molecules.[15,23−25] Thus, it has been questioned whether or not this species could have a sufficient lifetime to be observed experimentally until it was generated in ion beam experiments.[29,30] $H_3O\cdot(H_2O)_{3m}$ (for $m = 1-3$, at least) are charge-separated species with H_3O existing as a cation and the electron being located on the periphery of the water network.[15]

The structural diversity and complexity of the systems associated with solvated H is obvious. Mechanistic and nonadiabatic dynamics studies are still needed to understand all relevant processes. However, first and foremost, it is desirable to have full information about the ground PES for such systems and all accessible minima on it. This will facilitate further dynamics studies and the choice for appropriate small models in them. Here, we report on the ground PES of $H\cdot(H_2O)_n$ ($n = 1-4$) clusters. We address the question of their extremely diverse isomerism, stability, and electronic properties.

Methods

The search for the global minimum and the local minima isomer structures of the clusters is done with the new GEGA program. The original version of GEGA for operating solely on atomic clusters was reported previously.[9,10] A newly developed capability of operating on clusters using molecules as an operative subunit, as opposed to atoms, is now presented. The main difference between traditional GAs and GEGA is the use of ab initio gradient and geometry optimization for each cluster participating in the search. This way, the configurational space is sampled much more rapidly with the bias toward chemically relevant structures of local minima.

GEGA starts from generating an initial population of cluster geometries. First, structures are produced in a number quadruple the desired target size of the population. The coordinates of the atoms and molecules constituting the cluster are generated semirandomly within a Cartesian box as follows: The box size is chosen on the basis of the valence radii of atoms and approximate van der Waals radii of molecules forming the cluster and is scaled according to the user-defined cluster topology (the choice of compact, medium, and open). When coordinates are generated, the minimum allowed interunit distance is also observed, which is calculated for each unit pair on the basis of the aforementioned unit radii. For the constituent molecules, the geometries are preoptimized with CCSD(T)[31]/6-311++G**.[32] Rigid molecules are then given random orientations before joining the cluster. To enrich the population with structurally diverse genetic material, linear, planar, and 3-dimensional species are generated separately and deliberately. Ab initio single point energy calculations are then performed for all structures, and only the best 25% of individuals are preserved to form the initial population of the target size. The target size of the population is user-defined. The larger it is, the more accurate the search would be but to the expense of computer time. The optimal size of the population depends on the size of the system of interest. For $H\cdot(H_2O)_n$, it was chosen to be 10, 20, and 30, for $n = 2$, 3, and 4, respectively. For $n = 1$, the search for isomers was done manually.

All selected structures are then optimized to the nearest local minima on the ground PES. All degrees of freedom, including

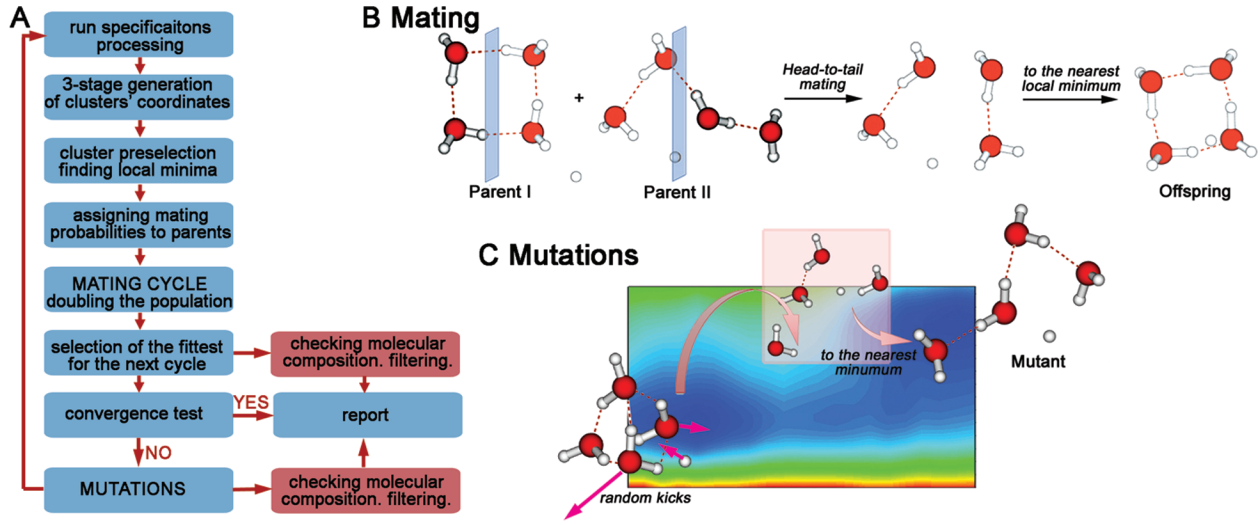

Figure 1. GEGA workflow (A) and GA operations on molecular clusters: mating (B) and mutation (C).

the internal degrees of freedom of the molecules, are varied during optimization. Vibrational frequency calculations follow geometry optimizations, and, if a saddle point is encountered, the normal modes of imaginary frequencies are followed until a minimum is found. The identified minima then start participating in the genetic algorithm procedure, where they are set to mate and to produce offspring and occasionally to mutate. Molecules are treated as unbreakable entities in the GA operations.

In the mating procedure, each cluster in the population is assigned a probability to mate on the basis of its fit, the total energy: the lower the energy, the greater is the probability. Two parent clusters are then randomly selected from the population on the basis of their mating probabilities. The algorithm utilizes the mating operator, where geometries of the parent clusters are cut with a randomly oriented cutting plane passing through the center of the mass of the cluster, and their geometric halves are combined to form a child cluster (Figure 1A). The combination is randomly chosen to be either simple or head-to-tail. The orientations of molecular units are preserved during combination. If a molecule in the cluster happens to be cut by the cutting plane, it is set to belong to one or the other half on the basis of the position of its center of mass. To ensure that the total number of cluster constituents of all types is the same, the cutting plane can be shifted so as to accept or discard extra atoms from either just parent II. This procedure allows combining geometric features of good structures with the hope of producing an even better offspring. The formed child is then optimized to the nearest local minimum. Both the parents and the offspring remain in the population. The mating continues until the size of the population is doubled. Subsequently, out of the structures of the same original molecular constitution (see below for the cases when this original constitution is not preserved), the new population of the original size is formed. Structures of new molecular composition are removed from the search and are reported to the user. The worst fit structures are stored in the database, which becomes available to the user. The lower-energy half is retained to continue with GA. Among the retained structures, it is possible to have both the original parents and the offspring.

After the mating cycle is over, and if the algorithm has not yet converged, 30% of the structures (having the worst fit in the population) are subjected to mutations. This atypically high mutation rate is explained by the nature of the mutation procedure in which only some of the species subjected to mutations actually become mutants. Mutations (Figure 1B) are random deformations of a cluster achieved by performing several kicks[3] on constituent atoms and, for molecules, the centers of mass; molecules are treated as rigid bodies during mutations. The total number of kicks per mutation is random, but it is equal to or smaller than half the total number of atoms/molecules in the cluster. If a particular kick causes a steric clash in the cluster, its magnitude is reduced to avoid the clash, and, if this does not help, it is assigned a new direction.

The purpose of the mutation procedure is to push the cluster across a barrier on the PES toward a new minimum. Mutants are then subjected to geometry optimization and frequency calculation until a local minimum is found. If kicks do not succeed in overcoming a barrier, the geometry optimization will take the cluster back to the original minimum. Because of this effect, the resulting effective mutation rate happens to be close to 10%. This apparent loss of computer time is a drawback; however, the use of geometry optimization still speeds up the GA search by 1−2 orders of magnitude as compared to GAs based on single point energy calculations. At the end of mutations, both the original structures and the mutants join the population, and the best individuals are again selected to carry on with the GA process. Mutations are incorporated in order to prevent the algorithm from getting stuck in a local minimum.

The mating and mutation cycle continues until the identified most stable structure stays the same for 20 iterations. When this happens, the algorithm is considered converged. The leading structure is very likely to be the global minimum, or at least a very stable local minimum, if the level of ab initio theory throughout the algorithm is adequate for the system at hand. The search is repeated three to five times for each cluster to ensure that the result is reproducible and is not an artifact of a particular GEGA run. If relevant, different cluster multiplicities should be interrogated separately. Here, all GEGA searches were done for doublets since it was demonstrated in the past that quadruplet states of these clusters are higher in energy. Finally, GEGA does not usually recognize the symmetry of the found isomers. The symmetry, if present, should be assigned manually during the a posteriori analysis.

As was mentioned, all degrees of freedom are varied during every geometry optimization during the search including the internal degrees of freedom of water molecules. This flexibility allows for bond breaking and forming and thus for the formation

of new molecular and atomic entities. In this way, the GEGA search does not prevent the new structural types from forming. However, GEGA in its current implementation does not branch the search onto several different ones if a new structural type is discovered. Instead, new structural types are removed from the search and are stored and reported to the user. At the end of the run, all structures, including those of new types, are sorted by their relative energies. Thus, GEGA has a bias toward clusters of the original constitution (here, it is H and $n$$H_2O$) and, to allow for a better sampling of the regions of configurational space corresponding to other compositions, additional GEGA searches are performed separately for all newly found cluster compositions. For the particular clusters considered here, two additional searches appeared to be necessary: for clusters consisting of H_2, OH, and $(n - 1)H_2O$ and for clusters consisting of H_3O and $(n - 1)H_2O$. If at any point in the search the population cannot maintain the size because of too many clusters being discarded, additional species are taken from the current database of minima that resulted from previous iterations. GEGA may completely fail if the original structural units are inappropriate, and thus, structures of other types are overwhelmingly prevalent on the ground PES, and there are not enough structures to carry on with the search.

In choosing the appropriate level of theory to go with the GEGA search, we first investigated the smallest species (n = 1) and found that DFT methods (B3LYP[32] and TPSSh[33]) with a fairly large basis set, 6-311++G**, provide reliable results for relative energies and geometries of these clusters. The large basis set is required for the adequate description of the weakly bound species. Thus, the GEGA search was done with both methods.

The found isomers were subsequently subjected to geometry refinement and vibrational frequency analysis at MP2[34] and CCSD(T) with 6-311++G** and aug-cc-pVTZ[35] basis sets. Single point energy calculations were further done at CCSD(T)/6-311++G(2df,2pd). All calculations were done with unrestricted methods, and the <S^2> value was 0.752 or less for all reported clusters indicating the minimal spin contamination and thus the single-reference character of the wave function. Additionally, CASSCF(n,m)[36]/6-311++G** calculations were performed in order to evaluate the nature of the cluster wave function. For all neutral clusters, and regardless of the size of the active space in CASSCF, the reference HF function was found to be highly dominant. The clusters are, therefore, not multiconfigurational, and the single reference methods used herein are valid. Natural bond order (NBO)[37] analysis was done at the B3LYP/6-311++G** level to assess the degree of charge transfer (if any) and the location of the radical character in the clusters. All ab initio calculations were done with Gaussian 09.[38]

Results and Discussion

A. Structure. *H·H₂O.* The structures of the global minimum and the low-lying local minima for this smallest cluster were identified manually without the use of GEGA. Structures are shown in Figure 2. Isomers **I** and **II** are the most stable structures on the PES. They consist of a H atom coordinated to H_2O in two possible ways. The distance to the coordinated H and its orientation relative to the H_2O vary significantly with the theoretical method. This indicates that the corresponding minima on the PES are shallow. For isomer **I**, depending on the method in use, the structure is either C_{2v} ($^2A_1$) or C_s ($^2A'$). For example, TPSSh predicts H to coordinate to H_2O at an almost right angle to the plane of the water molecule. MP2/aug-cc-pVTZ and B3LYP with either of the two basis sets predict the torsional angle to be ca. 127°, and MP2/6-311++G** predicts H to coordinate in a coplanar orientation with the H atoms of the water molecule (C_{2v}). Isomer **II** is of the C_s ($^2A'$) symmetry. Isomer **III**, C_s ($^2A'$), contains a H_2 molecule coordinated to the OH radical. For isomer **III**, there are several almost isoenergetic structures that differ slightly in the relative positions of the subunits. The PES is very flat in the corresponding region of the configurational space. Isomer **IV** is the hydronium radical, which is the species that received the most attention in recent studies.

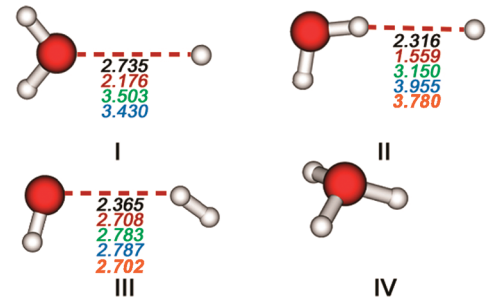

Figure 2. Isomers of H·H_2O and their geometries recomputed at various levels of theory: black, B3LYP/6-311++G**; red, TPSSH/6-311++G**; green, MP2/6-311+G**; blue, CCSD(T)/6-311++G**; orange, CASSCF. **IV** is a bound C_{3v} minimum at all levels, and so no specific geometric characteristics are shown.

Apparently, isomers **I**−**III** are weakly bound and, therefore, may present a complicated case for electronic structure methods especially if long-range charge transfer is involved. This smallest cluster, H·H_2O, was therefore used to check the performance of various theoretical methods for the studied clusters in general. Geometric features of the clusters computed at various levels of theory are reported in Figure 2. In Table 1, we show the total energies, the zero point energy corrections (ZPE), and the energy differences from the global minimum for the four found isomers as computed with various methods and basis sets. One may see that all methods uniformly predict isomers **I** and **II** to be almost isoenergetic so as to be difficult to decide which is the global minimum. Both **I** and **II** are van der Waals complexes, only weakly bound, that easily undergo a mutual rearrangement. For example, **I** converts to **II** at MP2 and CCSD(T) with the aug-cc-pVTZ basis set. Isomers **III** and **IV** appear 10−20 kcal/mol above the global minimum depending on the method. Dissociated clusters are only ca. 3 kcal/mol less stable than the global minimum. We managed to achieve the convergence of the CASSCF/6-311++G** calculations only when using different CAS active spaces for different isomers: (7,6), (5,6), and (3,4) for isomers **I**−**II**, **III**, and **IV**, respectively. For this reason, their relative energies are not reported at this level. However, **II**−**IV** are true minima on the PES, and their geometries are in agreement with those obtained with other methods (Figure 2). Isomer **I** is not a minimum and rearranges to **II** just as at MP2 and CCSD(T) levels with the aug-cc-pVTZ basis set. The Hartree−Fock configuration was always highly dominant in the CASSCF expansion showing a clear single reference character of the wave function. Because the predictions by various methods for relative energies and structural nature of isomers are consistent, for all larger clusters, we rely only on B3LYP/6-311++G** and MP2/6-311++G** calculations.

H·(H₂O)₂. Figure 3 shows the lowest energy isomers for H·$(H_2O)_2$, as found by GEGA//B3LYP/6-311++G** and as confirmed by GEGA//TPSSh/6-311++G**, and the distances to the weakly coordinated subunits in all structures. The types of structures and their relative energies remain approximately the same for these larger clusters as for the smaller cluster,

TABLE 1: Total Energies (in au), ZPE Values (in kcal/mol), and Energy Differences from the Global Minimum (in kcal/mol) for the Lowest Energy Isomers of $H\cdot H_2O$

method	isomer I	isomer II	isomer III	isomer IV
B3LYP/6-311++G**	−76.961019	−76.960978	−76.942411	−76.941157
	13.791	13.755	12.423	15.171
	0.0	0.02	11.71	11.08
TPSSH/6-311++G**	−76.952727	−76.951342	−76.938279	−76.927772
	14.561	13.696	12.672	13.873
	0.0	1.73	10.96	16.35
MP2/6-311++G**	−76.774785	−76.774796	−76.740915	−76.743568
	13.736	13.773	12.910	16.808
	0.0	−0.004	22.12	16.56
CCSD(T)/6-311++G**	−76.786486	−76.786507	−76.765560	−76.751688
	13.860	13.727	12.587	16.862
	0.0	0.14	14.40	18.83
B3LYP/aug-cc-pVTZ	−76.968523	−76.968750	−76.948904	−76.947707
	13.604	13.721	12.636	15.169
	0.0	0.02	13.28	11.50
MP2/aug-cc-pVTZ	rearranges to II	−76.829047	−76.792057	−76.796634
		13.728	12.857	16.199
			24.08 (from II)	17.87 (from II)
CCSD(T)/aug-cc-pVTZ	rearranges to II	−76.842493	−76.819012	−76.813424
		13.735	12.419	16.381
			16.04 (from II)	15.59 (from II)

$H\cdot H_2O$: the lowest energy isomers are $(H_2O)_2$ dimers with the radical H coordinated either to O (type **I**) or to H (type **II**) of one of the water molecules. The isomers of the next lowest energy type, **III**, contain H_2 coordinated to $OH\cdot H_2O$ in various ways, and these are ca. 10 kcal/mol higher in energy than the isomers of types **I** and **II**. The isomers of type **IV** containing the H_3O radical were found to be ca. 7 kcal/mol higher in energy than **I**. There are several isomers of each structural type as identified by GEGA. Here, the cluster types **III** and **IV** were found in the main GEGA run for $H\cdot(H_2O)_2$, were excluded from the search, and were reported. Subsequently, an additional run was performed for the $H_2\cdot(OH)\cdot(H_2O)$ composition, and for $H_3O\cdot(H_2O)$, it was found unnecessary.

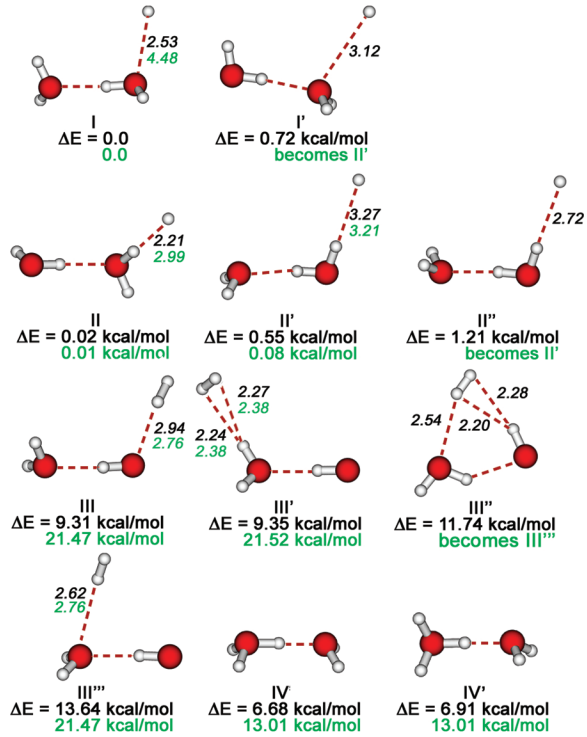

Figure 3. Isomers of $H\cdot(H_2O_2)_2$ found by GEGA//B3LYP/6-311++G** and refined by MP2/6-311++G**. Geometries and relative energies are shown at B3LYP/6-311++G** (black) and MP2/6-311+G** (green).

As is obvious in $H\cdot(H_2O)_2$ clusters and as becomes even more so for larger ones, overall, there appear to be many shallow minima on the PES of these systems. Some of these minima are also high in energy as compared to the global minimum. Clusters of types **III** and **IV** are examples of high-energy isomers as is also such species as $H-HOOH-H_2$ and $H_2-HOO-H_2$, which lie ca. 90 kcal/mol above the global minimum. The global minima themselves are weakly bound complexes prone to dissociation. Additionally, many minima differ among themselves only by the relative orientation of the H atoms on the water molecules that are not directly involved in the interfragment binding. The relative energies of such isomers can be within 1 kcal/mol from one another. All these features of the $H\cdot(H_2O)_2$ clusters make the search for the global minimum nontrivial and present a challenging case for the GEGA program.

$H\cdot(H_2O)_3$. The number of isomers grows very fast with the cluster size. As illustrated in Figure 4, for the $H\cdot(H_2O)_3$ cluster, there are many isomers of each structural type (**I**−**IV**). Additionally, almost all of the shown structures have isomers (not shown) that differ only by relative orientations of the dangling H atoms on water molecules. Among isomers of types **I** and **II**, there are two basic arrangements of the solvent water molecules. Water can form a triangular cluster and a H-bonded chain. H is then coordinated to these two motifs in various ways. Clusters containing a triangular $(H_2O)_3$ unit are the most stable species obviously maximizing the H bonding in the cluster. Similarly, for the isomers of type **III**, the triangular arrangement of $OH\cdot(H_2O)_2$ is preferred.

Clusters of types **I** and **II** are still the most stable. Clusters of type **III** are 12−15 kcal/mol higher in energy. Clusters of type **IV** are 9−13 kcal/mol higher in energy. Additionally, we found a fairly stable intermediate isomer named **I-II** in Figure 4, which can be classified as both **I** and **II**. We notice that the relative energies and the nature of the isomers do not change significantly when clusters increase in size.

In Figure 5, we show the found variations of the most stable isomers of types **I** and **II** containing a triangular arrangement of water molecules. The naming in Figure 5 is as follows: the

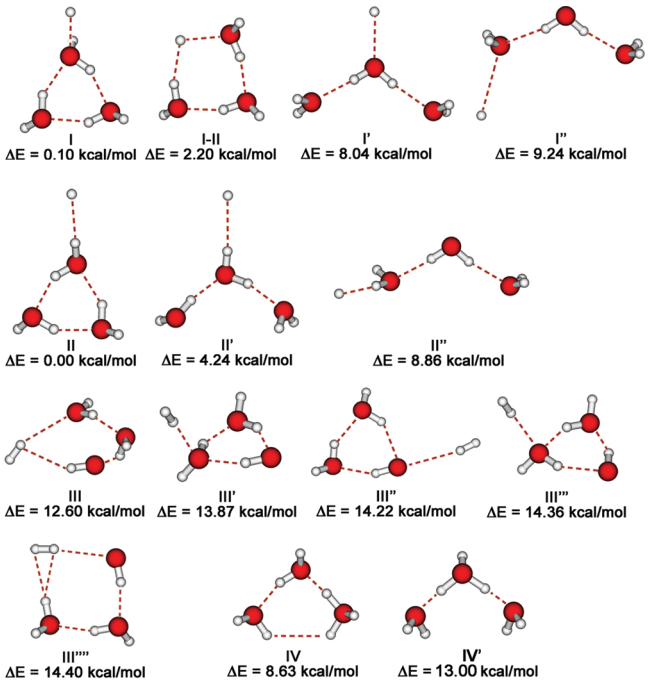

Figure 4. Selected isomers of $H\cdot(H_2O_2)_3$ found by GEGA//B3LYP/6-311++G** shown in order of structural type subgroup.

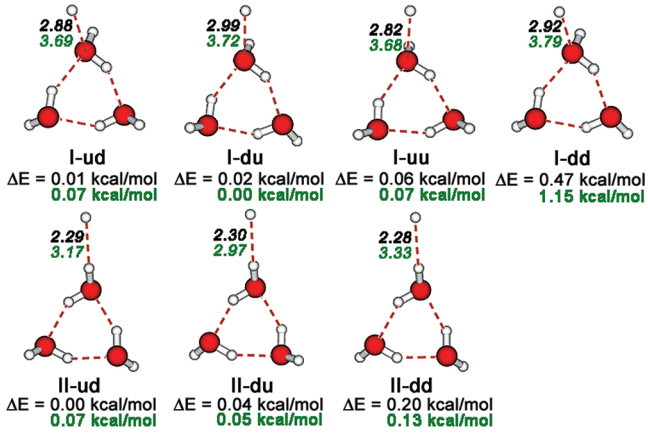

Figure 5. All triangular isomers of $H\cdot(H_2O_2)_3$ of types **I** and **II** found at B3LYP/6-311++G** (black) and refined at MP2/6-311++G** (green). The shown isomers that belong to the same family thermally interconvert, which makes them indistinguishable.

orientation of each water H atom pointing outward in the cluster is marked as "d" for down or as "u" for up with respect to the cluster plane and the coordinated H radical. The first thus marked H atom in the name belongs to the water molecule, which plays the role of H-bond acceptor to the water coordinating the H radical. The other dangling H atom is named next as it is next in line around the cycle.

One may see that these isomers are all found within 1 kcal/mol from one another. Additionally, we computed the barriers to the interconversion of structures of each type achieved through the flipping motion of dangling H atoms. All barriers appeared to be smaller than 1 kcal/mol, which is below the ZPE of these clusters. Hence, H flips are thermally allowed at room temperature, and these clusters are indistinguishable.

In this case, all these isomers shown in Figure 5 were successfully found by GEGA, and no other isomers of these two types were found upon subsequent manual checking. In general, however, GEGA may have trouble finding all structures that differ only slightly, for example, by the relative orientations of dangling H atoms on water molecules. Missing isomers have to be checked by hand. This does not result from an innate inability of GEGA to find such isoenergetic isomers but does result rather from the ease with which these isomers interconvert. To automatically find all such species, the search would have to be longer, and the GA population would probably have to be even larger. We found that at this point it would be faster to check the missing conformers manually instead of continuing the GEGA search. This feature of GEGA is a minor deficiency of which the user needs to be aware.

H·(H₂O)₄. Starting with the clusters containing four water molecules, the total number of found isomers becomes almost unmanageable. Importantly, however, the nature (**I**−**IV**) and the relative energies of typical isomers are again preserved. **I** and **II** are the global minima. There are several isomers of intermediate nature, **I-II**, where both coordination modes for the H radical are simultaneously realized. **III** and **IV** lie 7−13 kcal/mol higher in energy. Clusters of types **III** and **IV** were found in the main GEGA search, and then their families were expanded in additional separate searches. In Figure 6, we show assorted representative isomers.

For each group of structures (**I**−**IV**), there are also several subgroups. For example, there are species of types **I** and **II** containing a square arrangement of water molecules (most stable), a triangular arrangement with one water coordinated to the vertex of the triangle (on average, 7−10 kcal/mol higher in energy), a completely open chain of four water molecules (ca. 20 kcal/mol higher in energy), and a closed, tetrahedron-like structure with a missing vertex (ca. 7 kcal/mol higher in energy than the global minimum). Among those subgroups, there are also many more isoenergetic structures that differ among themselves by relative orientations of the H atoms on water molecules participating in both H bonding and dangling. For example, for the structure **I** with the most favorable square arrangement of the four water molecules, there is a total of eight possible ways to arrange the dangling H atoms. Although not all of these structures are shown in Figure 6, they have been explored, and we identified which ones have the lowest energies within their corresponding subgroups.

In Figure 7, we show only the most stable, square structures of types **I** and **II** and all the existing isomers thereof. The naming in Figure 7 is analogous to that in Figure 5. Not all possible ways to arrange dangling H atoms correspond to minima on the PES. Some of them dissociate, and some convert to other isomers during geometry optimization. For example, the isomer **I-ddd** does not exist; it converts to **I-dud**. A total of six minima were found (Figure 7). All of them were found by GEGA, and the ones that seemed to be missing were checked manually and were identified as nonexistent. In reality, all the isomers of the same type correspond to just one structure because the ZPE takes them above the barriers for the H-flip motions thus eliminating the structural differences. These barriers were computed to be less than 1 kcal/mol.

As for the performance of GEGA for this larger cluster, we conclude that it was remarkably successful. However, in general, with larger cluster size, high-energy isomers corresponding to shallow minima on the PES are harder to catch. As a result, the saturation of the library of found isomers with those high-energy structures is relatively slow. This is due to both the shallowness of those minima and the sheer number of low-energy isomers whose presence in the population is overwhelming and becomes more so as the search progresses. Low-energy structures have many more chances to pass their structural information to the

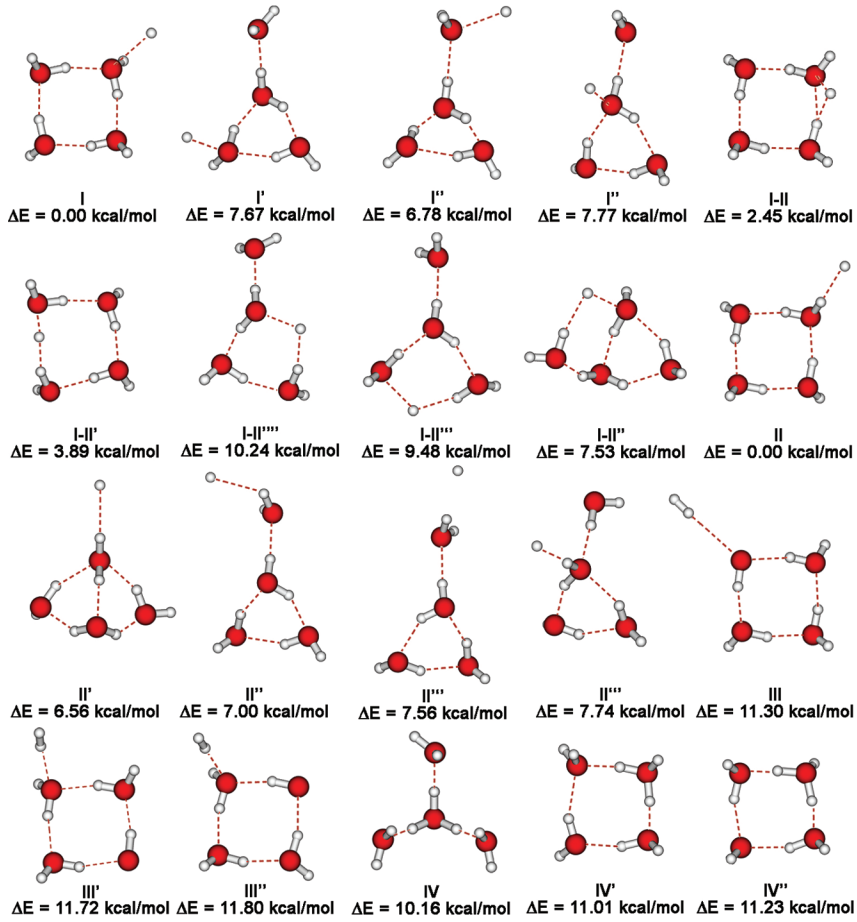

Figure 6. Selected isomers of $H^{\bullet}(H_2O_2)_4$ found by GEGA//B3LYP/6-311++G** shown in order of structural type subgroup. For isomers of types **III** and **IV**, only very few of the found structures are shown. The total number of isomers becomes almost unmanageable at this cluster size.

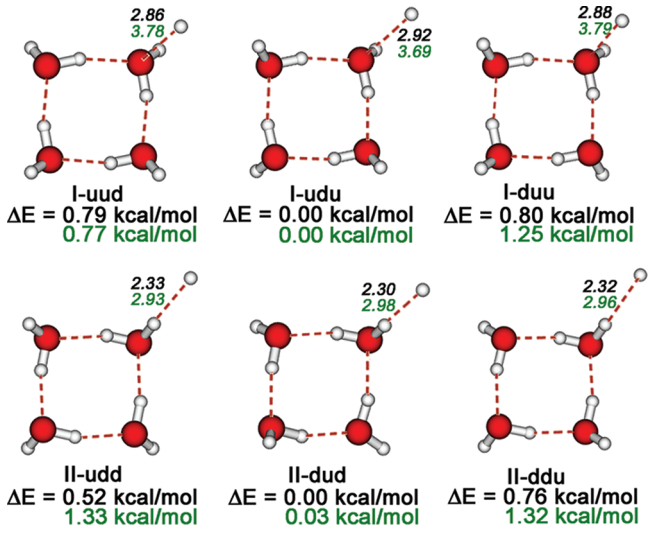

Figure 7. All square isomers of $H^{\bullet}(H_2O_2)_4$ of types **I** and **II** found at B3LYP/6-311++G** (black) and refined at MP2/6-311++G** (green). The shown isomers that belong to the same family thermally interconvert, which makes them indistinguishable.

offspring. In contrast, high-energy isomers are discarded in the selection process and thus have no chance of being extensively sampled.

B. Electronic Properties. From the structure of the found cluster types, it is fairly obvious where the radical character is located within each cluster. To confirm this, in Table 2, we show the charges on selected atoms computed using the natural population analysis part of the NBO code. For the isomers of types **I** and **II**, in clusters of all considered sizes, the unpaired electron is always on uncharged H, and the partial charge transfer is only minor. For clusters of type **III**, the radical character is always on OH. In the clusters of type **IV**, the H_3O unit is the carrier of the radical character in the smallest clusters ($n = 1, 2$). However, H_3O acquires a partial positive charge as the cluster grows and approaches the limit of solvated H_3O^+ and solvated electron. The unpaired electron becomes delocalized over the entire cluster for $n = 3, 4$. This is in agreement with predictions for other clusters of this type.[15] Figure 8 shows the highest occupied molecular orbitals (HOMOs) in all clusters of type **IV** illustrating the migration of the radical character from H_3O to the periphery of the cluster as the cluster grows in size.

The character of the wave function for all clusters is single-reference with the HF configuration being unequivocally

TABLE 2: NPA/B3LYP/6-311++G//B3LYP/6-311++G** Charges on Selected Groups of Atoms for the Lowest-Energy Isomers of Each Type**

type	n in $H^{\bullet}(H_2O)_n$	charge, e	type	n in $H^{\bullet}(H_2O)_n$	charge, e
I	1	$Q(H) = -0.0001$	**II**	1	$Q(H) = 0.0002$
	2	$Q(H) = -0.0001$		2	$Q(H) = 0.0003$
	3	$Q(H) = -0.0028$		3	$Q(H) = 0.0002$
	4	$Q(H) = -0.0042$		4	$Q(H) = 0.0019$
III	1	$Q(H_2) = 0.0047$ $Q(OH) = -0.0047$	**IV**	1	$Q(H_3O) = 0.0000$
	2	$Q(H_2) = -0.0064$ $Q(OH) = -0.0102$		2	$Q(H_3O) = 0.0365$
	3	$Q(H_2) = -0.0027$ $Q(OH) = -0.1156$		3	$Q(H_3O) = 0.4686$
	4	$Q(H_2) = -0.0069$ $Q(OH) = -0.0042$		4	$Q(H_3O) = 0.6436$

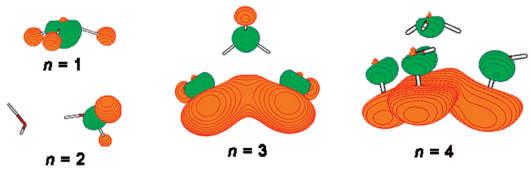

Figure 8. The HOMOs in the lowest-energy clusters of type **IV**.

dominant. However, when an extra electron is vertically removed from the neutral clusters at their optimized geometries, all cationic clusters except for isolated H_3O become open-shell singlets with the wave function consisting of two configurations. For clusters of types **I**−**III**, this means that the ejected electron originates not from the original radical carrier (H or OH) but from water. This is in accord with the VDEs for isolated H, OH, H_2, and H_2O being 13.6, 13.4, 16.4, and 12.6 eV, respectively, as computed at CCSD(T)/6-311++G**, that is, the VDE for water is the lowest of all. This correlation with VDEs of isolated species is an additional indication that the complexes **I**−**III** are only weakly bound for all considered cluster sizes. Clusters of type **IV** are bound more strongly. Yet, it appears that the first VDE corresponds to the electron leaving from a molecular orbital (MO) other than the HOMO in the neutral clusters making the wave function of the cation two-reference.

Here, we do not attempt to calculate VDEs and to explicate the electronic properties any further, however. Of additional fundamental interest would also be higher VDEs and various electron detachment channels, electronic excitation energies, and nature of the excited states especially those entailing charge transfer, the topography of excited states' PESs, and conical intersections. To provide a quality assessment of these properties, multireference calculations sometimes in conjunction with quantum or semiclassical dynamics simulations would have to be carried out. This is beyond the scope of the present study, whose purpose is the extensive exploration of the ground PES of the studied clusters.

Conclusions

We present a new algorithm (GEGA) for the search of the global and low-energy local minima on the potential energy surfaces of clusters formed by atoms and molecules. GEGA is similar in spirit to its original version developed for pure atomic clusters. It combines the features of genetic algorithm strategy for exchange of structural information between clusters, selection of the fittest, and mutations of low-fit species. It also takes advantage of ab initio gradient-following geometry optimization and vibrational frequency analysis used for the location of local minima throughout the search. Molecules are treated as intact units during GA operations. However, during ab initio calculations, their internal degrees of freedom are allowed to be varied.

In this work, we successfully applied GEGA to the structural search on the PES of $H\cdot(H_2O)_n$ ($n = 1-4$) clusters. We found that these systems present a particular challenge for GEGA because of many shallow, isoenergetic, and prone to dissociation minima on the PES. The large number of isomers near the global minimum, in terms of their energies, leads to the early saturation of the population with these low-energy structures. This complicates the sampling of higher regions of the PES. Furthermore, the molecular structure of the isomers is not preserved in some of the isomers, specifically, isomers of types **III** and **IV** (for example, in Figure 2). As a result, the initial choice for the constituents, H and nH_2O, appeared to be insufficient. GEGA was capable of revealing the new structural types but had a bias toward clusters formed by H and nH_2O. To increase the sampling of the corresponding regions of configurational space, additional GEGA searches were performed with different choices for the cluster components. Despite the complications, overall GEGA performed exceptionally well in these searches. The results were checked through performing multiple runs of GEGA at two different levels of theory, manual checking for structures seemingly missing from the search, and subsequent refinement of structures and total energies at higher levels of theory.

We found that all clusters have four basic structural families. Structures of type **I** have a water cluster and the H radical coordinated to the O atom of one of the water molecules. Structures of type **II** have a water cluster and the H radical coordinated to the H atom of one of the water molecules. Species **I** and **II** share the title of the global minimum. They are also weakly bound, and species completely dissociated to H and a water cluster are only 3 kcal/mol higher in energy. There are a few intermediate structures of type **I**-**II**, where both coordination modes are accomplished in a single cluster. Further, there are structures of type **III** that contain H_2, the OH radical, and a cluster formed by the remaining water molecules. Finally, there are structures of type **IV** containing a hydronium radical H_3O coordinated to a water cluster. The radical character in clusters of type **IV** distributes over the entire cluster as the cluster grows in size approaching the limit of charge-separated solvated H_3O^+ and solvated electron. Clusters of types **III** and **IV** are ca. 10 kcal/mol higher in energy than the global minima. The four structural types and relative energies of clusters belonging to certain types are persistent through all considered cluster sizes.

This work contributes to the knowledge about the ground PES and the rich isomerism of $H\cdot(H_2O)_n$ clusters. This is essential for the fundamental understanding of complex processes related to the presence of solvated H radical and solvated electron in various natural circumstances ranging from enzymatic catalysis to photochemistry of water.

Acknowledgment. This work was supported by the University of California, Los Angeles.

References and Notes

(1) (a) Metropolis, N.; Ulam, S. *J. Am. Stat. Assoc.* **1949**, *44*, 335–341. (b) Metropolis, N.; Rosenbluth, A. W.; Rosenbluth, M. N.; Teller, A. H.; Teller, E. *J. Chem. Phys.* **1953**, *21*, 1087. (c) Manno, I. *Introduction to the Monte Carlo Method*; Akadémiai Kiadó: Budapest, Hungary, 1999. (d) Kirkpatrick, S.; Gelatt, C. D.; Vecchi, M. P. *Science* **1983**, *220*, 671.

(2) (a) Wales, D. J.; Doye, J. P. K. *J. Phys. Chem. A* **1997**, *101*, 5111. (b) Doye, J. P. K.; Wales, D. J.; Miller, M. *J. Chem. Phys.* **1998**, *109*, 8143. (c) Back, T. *Evolutionary Algorithm in Theory and Practice: Evolutionary Programming, Genetic Algorithms*; Oxford University Press: Oxford, United Kingdom, 1990.

(3) Saunders, M. *J. Comput. Chem.* **2004**, *25*, 621.

(4) Lloyd, L. D.; Johnston, L. *Chem. Phys.* **1998**, *236*, 107.

(5) Berg, B.; Neuhaus, T. *Phys. Lett. B* **1991**, *267*, 249.

(6) Goedecker, S. *J. Chem. Phys.* **2004**, *120*, 9911.

(7) Call, S. T.; Zubarev, D.; Yu. Boldyrev, A. I. *J. Comput. Chem.* **2007**, *28*, 1177–1186.

(8) (a) Deaven, D. M.; Ho, K. M. *Phys. Rev. Lett.* **1995**, *75* (2), 288–291. (b) Gregurick, S. K.; Alexander, M. H.; Hartke, B. *J. Chem. Phys.* **1996**, *104*, 2684.

(9) (a) Alexandrova, A. N.; Boldyrev, A. I. J. *Chem. Theory Comput.* **2005**, *1*, 566–576. (b) Alexandrova, A. N.; Boldyrev, A. I.; Fu, Y.-J.; Yang, X.; Wang, X.-B.; Wang, L.-S. *J. Chem. Phys.* **2004**, *121*, 5709−1–11.

(10) (a) Zubarev, D. Yu.; Averkiev, B. B.; Zhai, H.-J.; Wang, L.-S.; Boldyrev, A. I. *Phys. Chem. Chem. Phys.* **2008**, *10*, 257–267. (b) Zhai, H.-J.; Averkiev, B. B.; Zubarev, D. Yu.; Wang, L.-S.; Boldyrev, A. I. *Angew. Chem., Int. Ed.* **2007**, *46*, 4277–4280. (c) Zhai, H. J.; Wang, L.-S.; Alexandrova, A. N.; Boldyrev, A. I. *J. Phys. Chem. A* **2003**, *107*, 9319. (d) Alexandrova, A. N.; Boldyrev, A. I.; Zhai, H. J.; Wang, L.-S. *Coord. Chem. Rev.* **2006**, *250*, 2811. (e) Cui, L. F.; Huang, X.; Wang, L.-M.; Zubarev, D. Yu.; Boldyrev, A. I.; Li, J.; Wang, L. S. *J. Am. Chem. Soc.* **2006**, *128*,

8390–8391. (f) Alexandrova, A. N.; Koyle, E.; Boldyrev, A. I. *J. Mol. Model.* **2006**, *12*, 569–576. (g) Zubarev, D. Y.; Alexandrova, A. N.; Boldyrev, A. I.; Ciu, L.-F.; Wang, L.-S. *J. Chem. Phys.* **2006**, *124*, 124305. (h) Wang, L.-M.; Huang, W.; Wang, L. S.; Averkiev, B. B.; Boldyrev, A. I. *J. Chem. Phys.* **2009**, *130*, 134303-1-7. (i) Averkiev, B. B.; Call, S.; Boldyrev, A. I.; Wang, L. M.; Huang, W.; Wang, L. S. *J. Phys. Chem. A* **2008**, *112*, 1873–1879. (j) Zubarev, D. Y.; Li, J.; Wang, L.-S.; Boldyrev, A. I. *Inorg. Chem.* **2006**, *45*, 5269–5271. (k) Averkiev, B. B.; Zubarev, D. Y.; Wang, L.-M.; Huang, W.; Wang, L.-S.; Boldyrev, A. I. *J. Am. Chem. Soc.* **2008**, *130*, 9248–9250. (l) Sergeeva, A. P.; Zubarev, D. Y.; Zhai, H.-J.; Boldyrev, A. I.; Wang, L.-S. *J. Am. Chem. Soc.* **2008**, *130*, 7244–7246. (m) Wang, L.-M.; Huang, W.; Averkiev, B. B.; Boldyrev, A. I.; Wang, L.-S. *Russ. J. Gen. Chem.* **2008**, *78*, 769–773. (n) Wang, L.-M.; Huang, W.; Averkiev, B. B.; Boldyrev, A. I.; Wang, L.-S. *Angew. Chem., Int. Ed.* **2007**, *46*, 4550–4553. (o) Tiznado, W.; Perez-Peralta, N.; Islas, R.; Toro-Labbe, A.; Ugalde, J. M.; Merino, G. *J. Am. Chem. Soc.* **2009**, *131*, 9426–9431. (p) Yao, W.-Y.; Guo, J.-C.; Lu, H.-G.; Li, S.-D. *J. Phys. Chem. A* **2009**, *113*, 2561–2564. (q) Fernandez-Lima, F. A.; VilelaNeto, O. P.; Pimentel, A. S.; Ponciano, C. R.; Pacheco, M. A. C.; Chaer Nascimento, M. A.; da Silviera, E. F. *J. Phys. Chem. A* **2009**, *113*, 1813–1821. (r) Ortega-Moo, C.; Cervantes, J.; Mendez-Rojas, M. A.; Pannell, K. H.; Merino, G. *Chem. Phys. Lett.* **2010**, *490*, 1–3.

(11) Hammes-Schiffer, S. *Acc. Chem. Res.* **2001**, *34*, 273–281.

(12) Kim, S. Y.; Hammes-Schiffer, S. *J. Chem. Phys.* **2003**, *119*, 4389–4398.

(13) Kirchner, B.; Stubbs, J.; Marx, D. *Phys. Rev. Lett.* **2002**, *89*, 215901-1-4.

(14) Kloepfer, J. A.; Vilchiz, V. H.; Lenchenkov, V. A.; Chen, X.; Bradforth, S. E. *J. Chem. Phys.* **2002**, *117*, 766–778.

(15) (a) Sobolewski, A. J.; Domcke, W. *Phys. Chem. Chem. Phys.* **2002**, *4*, 4–10. (b) Sobolewski, A. J.; Domcke, W. *J. Phys. Chem.* **2002**, *106*, 4158–4167.

(16) Han, P.; Bartels, D. M. *J. Phys. Chem.* **1992**, *96*, 4899–4906.

(17) Marin, T. W.; Jonah, C. D.; Bartels, D. M. *J. Phys. Chem. A* **2005**, *109*, 1843–1848.

(18) Renault, J. P.; Vuilleumier, R.; Pommeret, S. *J. Phys. Chem. A* **2008**, *112*, 7027–7034.

(19) Shiraishi, H.; Sunaryo, G. R.; Ishigure, K. *J. Phys. Chem.* **1994**, *98*, 5164–5173.

(20) Erdey-Gruz, T. *Transport Phenomena in Aqueous Solutions*; Adam Hilger: London, 1974.

(21) Marsalek, O.; Frigato, T.; VandeVondele, J.; Bradforth, S. E.; Schmidt, B.; Schuette, C.; Jungwirth, P. *J. Phys. Chem. B* **2010**, *114*, 915–920.

(22) Neumann, S.; Eisfeld, W.; Sobolewski, A. J.; Domcke, W. *Phys. Chem. Chem. Phys.* **2004**, *6*, 5297–5303.

(23) Talbi, D.; Saxon, R. P. *J. Chem. Phys.* **1991**, *15*, 2376–2387.

(24) Ermoshin, V. A.; Sobolewski, A. J.; Domcke, W. *Chem. Phys. Lett.* **2002**, *356*, 556–562.

(25) Niblaeus, K. S. E.; Roos, B. O.; Siegbahn, P. E. M. *Chem. Phys.* **1977**, *25*, 207–213.

(26) Sobolewski, A. J.; Domcke, W. *Phys. Chem. Chem. Phys.* **2007**, *9*, 3818–3829.

(27) Muguet, F. F.; Gelabert, H.; Gauduel, Y. *J. Chem. Phys.* **1996**, *93*, 1808.

(28) Yang, M.; Zhang, D. H.; Collins, M. A.; Lee, S.-Y. *J. Chem. Phys.* **2001**, *115*, 174–178.

(29) Gellene, G. I.; Porter, R. F. *J. Chem. Phys.* **1984**, *81*, 5570.

(30) (a) Cizek, J. *Adv. Chem. Phys.* **1969**, *14*, 35. (b) Purvis, G. D., III; Bartlett, R. J. *J. Chem. Phys.* **1982**, *76*, 1910. (c) Scuseria, G. E.; Janssen, C. L.; Schaefer, H. F., III. *J. Chem. Phys.* **1988**, *89*, 7382. (d) Scuseria, G. E.; Schaefer, H. F., III. *J. Chem. Phys.* **1989**, *90*, 3700. (e) Pople, J. A.; Head-Gordon, M.; Raghavachari, K. J. A. *J. Chem. Phys.* **1987**, *87*, 5968. (f) Knowles, P. J.; Hampel, C.; Werner, H.-J. *J. Chem. Phys.* **1993**, *99*, 5219. (g) Raghavachari, K.; Trucks, G. W.; Pople, J. A.; Head-Gordon, M. *Chem. Phys. Lett.* **1989**, *157*, 479.

(31) (a) Clark, T.; Chandrasekhar, J.; Spitznagel, G. W.; Schleyer, P. v. R. *J. Comput. Chem.* **1983**, *4*, 294–301. (b) Frisch, M. J.; Pople, J. A.; Binkley, J. S. *J. Chem. Phys.* **1984**, *80*, 3265–3269.

(32) (a) Parr, R. G.; Yang, W. *Density-functional theory of atoms and molecules*; Oxford University Press: Oxford, United Kingdom, 1989. (b) Becke, A. D. *J. Chem. Phys.* **1993**, *98*, 5648. (c) Perdew, J. P.; Chevary, J. A.; Vosko, S. H.; Jackson, K. A.; Pederson, M. R.; Singh, D. J.; Fiolhais, C. *Phys. Rev. B* **1992**, *46*, 6671.

(33) Tao, J. M.; Perdew, J. P.; Staroverov, V. N.; Scuseria, G. E. *Phys. Rev. Lett.* **2003**, *91*, 146401.

(34) (a) Head-Gordon, M.; Pople, J. A.; Frisch, M. J. *Chem. Phys. Lett.* **1988**, *153*, 503. (b) Frisch, M. J.; Head-Gordon, M.; Pople, J. A. *Chem. Phys. Lett.* **1990**, *166*, 275. (c) Frisch, M. J.; Head-Gordon, M.; Pople, J. A. *Chem. Phys. Lett.* **1990**, *166*, 281.

(35) (a) Dunning, T. H., Jr. *J. Chem. Phys.* **1989**, *90*, 1007–23. (b) Kendall, R. A.; Dunning, T. H., Jr.; Harrison, R. J. *J. Chem. Phys.* **1992**, *96*, 6796–806. (c) Woon, D. E.; Dunning, T. H., Jr. *J. Chem. Phys.* **1993**, *98*, 1358–71. (d) Peterson, K. A.; Woon, D. E.; Dunning, T. H., Jr. *J. Chem. Phys.* **1994**, *100*, 7410–15. (e) Wilson, A. K.; van Mourik, T.; Dunning, T. H., Jr. *J. Mol. Struct. (THEOCHEM)* **1996**, *388*, 339–49.

(36) (a) Hegarty, D.; Robb, M. A. *Mol. Phys.* **1979**, *38*, 1795–812. (b) Eade, R. H. A.; Robb, M. A. *Chem. Phys. Lett.* **1981**, *83*, 362–68. (c) Schlegel, H. B.; Robb, M. A. *Chem. Phys. Lett.* **1982**, *93*, 43–46. (d) Bernardi, F.; Bottini, A.; McDougall, J. J. W.; Robb, M. A.; Schlegel, H. B. *Faraday Symp. Chem. Soc.* **1984**, *19*, 137–47. (e) Frisch, M. J.; Ragazos, I. N.; Robb, M. A.; Schlegel, H. B. *Chem. Phys. Lett.* **1992**, *189*, 524–28. (f) Yamamoto, N.; Vreven, T.; Robb, M. A.; Frisch, M. J.; Schlegel, H. B. *Chem. Phys. Lett.* **1996**, *250*, 373–78.

(37) (a) Carpenter, J. E.; Weinhold, F. *J. Mol. Struct. (THEOCHEM)* **1988**, *169*, 41–62. (b) Carpenter, J. E. Ph.D. Thesis, University of Wisconsin, Madison, WI, 1987. (c) Foster, J. P.; Weinhold, F. *J. Am. Chem. Soc.* **1980**, *102*, 7211–7218. (d) Reed, A. E.; Weinhold, F. *J. Chem. Phys.* **1983**, *78*, 4066–4073. (e) Reed, A. E.; Curtiss, L. A.; Weinhold, F. *Chem. Rev.* **1988**, *88*, 899–926.

(38) Frisch, M. J.; Trucks, G. W.; Schlegel, H. B.; Scuseria, G. E.; Robb, M. A.; Cheeseman, J. R.; Montgomery, J. A., Jr.; Vreven, T.; Kudin, K. N.; Burant, J. C.; Millam, J. M.; Iyengar, S. S.; Tomasi, J.; Barone, V.; Mennucci, B.; Cossi, M.; Scalmani, G.; Rega, N.; Petersson, G. A.; Nakatsuji, H.; Hada, M.; Ehara, M.; Toyota, K.; Fukuda, R.; Hasegawa, J.; Ishida, M.; Nakajima, T.; Honda, Y.; Kitao, O.; Nakai, H.; Klene, M.; Li, X.; Knox, J. E.; Hratchian, H. P.; Cross, J. B.; Bakken, V.; Adamo, C.; Jaramillo, J.; Gomperts, R.; Stratmann, R. E.; Yazyev, O.; Austin, A. J.; Cammi, R.; Pomelli, C.; Ochterski, J. W.; Ayala, P. Y.; Morokuma, K.; Voth, G. A.; Salvador, P.; Dannenberg, J. J.; Zakrzewski, V. G.; Dapprich, S.; Daniels, A. D.; Strain, M. C.; Farkas, O.; Malick, D. K.; Rabuck, A. D.; Raghavachari, K.; Foresman, J. B.; Ortiz, J. V.; Cui, Q.; Baboul, A. G.; Clifford, S.; Cioslowski, J.; Stefanov, B. B.; Liu, G.; Liashenko, A.; Piskorz, P.; Komaromi, I.; Martin, R. L.; Fox, D. J.; Keith, T.; Al-Laham, M. A.; Peng, C. Y.; Nanayakkara, A.; Challacombe, M.; Gill, P. M. W.; Johnson, B.; Chen, W.; Wong, M. W.; Gonzalez, C.; Pople, J. A. *Gaussian 03*, revision C.02; Gaussian, Inc.: Wallingford, CT, 2004.

JP1092543